Targeted gene transfection from microbubbles into vascular smooth muscle cells using focused, ultrasound-mediated delivery

Linsey C. Phillips[1], **Alexander L. Klibanov**[2], **Brian R. Wamhoff**[2,3,*], and **John A. Hossack**[1,*]

[1] Department of Biomedical Engineering, University of Virginia, Charlottesville, VA

[2] Department of Medicine, Cardiovascular Division, University of Virginia, Charlottesville, VA

[3] Robert M. Berne Cardiovascular Research Center, University of Virginia, Charlottesville, VA

Abstract

We investigate a method for gene delivery to vascular smooth muscle cells using ultrasound triggered delivery of plasmid DNA from electrostatically coupled cationic microbubbles. Microbubbles carrying reporter plasmid DNA were acoustically ruptured in the vicinity of smooth muscle cells *in vitro* under a range of acoustic pressures (0–950 kPa) and pulse durations (0–100 cycles). No effect on gene transfection or viability was observed from application of microbubbles, DNA, or ultrasound alone. Microbubbles in combination with ultrasound (500 kPa, 1MHz, 50 cycle bursts at a Pulse Repetition Frequency [PRF] of 100 Hz) significantly reduced viability both with DNA (53 +/− 27%) and without (19 +/− 8%). Maximal gene transfection (~1% of cells) occurred using 50 cycle, 1 MHz pulses at 300 kPa which resulted in 40% viability of cells. We demonstrated that we can locally deliver DNA to vascular smooth muscle cells *in vitro* using microbubble carriers and focused ultrasound.

Keywords

contrast agents; gene delivery; sonoporation; ultrasound

Introduction

The need for localized cardiovascular therapy has led to a variety of delivery techniques such as viral vectors, liposome agents, and drug-eluting polymers. Although gene delivery is efficient with some viral vectors, they are associated with greater risks as compared to naked DNA (Mayer and Bekeredjian 2008). Ultrasonic contrast agents, such as lipid coated microbubbles, have been under investigation as gene or drug delivery agents (Unger et al. 2001; Unger et al. 2004; Ferrara et al. 2007). Microbubbles circulate in the bloodstream, and serve as acoustic imaging agents as well as cardiovascular delivery agents (Lawrie et al. 2000). Furthermore, they can be ruptured in localized regions of interest through ultrasound destruction. For more than a decade it has been known that low frequency ultrasound enhances gene transfection to cultured cells (Kim et al. 1996). The addition of cavitation nuclei increases

gene transfection even further (Greenleaf et al. 1998). Unger et al. showed that the addition of cationic liposomes enhance ultrasound induced gene transfection *in vitro* (Unger et al. 1997) and *in vivo* (Anwer et al. 2000). Although the exact mechanism is not fully understood, the process by which ultrasound enhances reagent delivery through transient pore formation in the cell membrane is generally termed sonoporation. This process may occur due to jetting of gas out of the bubble or shear forces incurred during oscillation which lead to pore formation (Wu et al. 2002; Meijering et al. 2009). Both *in vivo* and *in vitro* studies have shown that microbubbles in combination with ultrasound enhance gene transfection (Christiansen et al. 2003; Rahim et al. 2006a).

The ultrasound conditions required to induce gene transfection are generally in the lower frequency range between 0.5–5MHz and transfection is enhanced with increasing acoustic pressure (Rahim et al. 2006b; Meijering et al. 2007). Previous studies have shown that peak negative pressure and similarly, pulse length, and duty cycle can affect the efficiency of gene transfection (Feril et al. 2006; Rahim et al. 2006b; Meijering et al. 2007; Ren et al. 2008). Although gene transfection increases with increasing acoustic pressure so too does cell death (Guzman et al. 2001a; Miller et al. 2003; Duvshani-Eshet et al. 2006; Karshafian et al. 2009). Many of these studies have investigated ultrasound parameters on drug or gene delivery and cell viability *in vitro*. Each study uses a different experimental design which in turns makes direct comparison and estimation of *in vivo* results challenging. To complicate matters further, the cell types used in these *in vitro* studies are often not vascular cells. Some cell lines are known to be more easily transfectable than others, such as Hela cells (Feril et al. 2006). Acoustic parameters for optimal gene delivery to vascular smooth muscle cells have not yet been determined.

Due to their ability to circulate in the bloodstream next to vessel walls, microbubbles may be exploited for cardiovascular therapy. In particular, a need exists for localized drug or gene therapy to stented vessel walls following angioplasty. In response to injury (e.g. following angioplasty or stenting), cells from the artery wall, primarily smooth muscle cells, proliferate into the intima, resulting in restenosis (Owens et al. 2004). Drug eluting stents have been developed to deliver localized drugs, however they have been associated with complications (Eisenstein et al. 2007), and an increased risk of late thrombosis or death (Camenzind et al. 2007; Byrne et al. 2009). New anti-proliferative therapies are needed to locally prevent neointimal restenosis while also reducing the risk of complications. This work investigates the use of cationic microbubble carriers of plasmid DNA to locally treat smooth muscle cells. Localized, anti-proliferative treatment of vascular smooth muscle cells will aid in the prevention of restenosis.

Methods

Cell Culture

Acoustically transparent Opticell flasks (Biocrystal, Westerville, OH) were coated with fibronectin (Invitrogen, Carlsbad, CA) for 24 hours prior to plating of any cells. Rat aortic vascular smooth muscle cells were plated at a density of 1.0×10^4 cells/cm^2 and cultured in growth (10% bovine serum) media (DMEM/F12, Gibco, Grand Island, NY) in an incubator at 37°C and 5% CO_2, as previously described (Orr et al. 2008). Cells were cultured for 24 hours to reach 70% confluency before experimentation.

Microbubble and Plasmid Construction and Conjugation

A plasmid construct composed of a cytomegalovirus (CMV) promoter and red fluorescent protein (RFP) encoding gene was chosen to allow for simple detection of successful gene transfection due to its strong red fluorescent emission in cells. Cationic lipid microbubbles

were formed by self-assembly as described previously (Christiansen et al. 2003). An aqueous micellar mixture of distearoyl phosphatidylcholine (2 mg/ml) (Avanti Lipids, Alabaster, AL), polyethylene glycol (PEG) stearate (2 mg/ml) (Sigma Chemical Co., St. Louis, MO), used to extend *in vivo* lifetime, and distearoyl trimethylammonium propane (0.4 mg/ml) (Avanti Polar Lipids, Alabaster, AL) was sonicated while sparging decafluorobutane gas (Flura, Newport, TN, USA). Microbubbles were separated from unreacted components by centrifugal flotation. Microbubble size and concentration were measured by electrozone sensing on a Coulter counter (Multisizer 3, Beckman Coulter, Brea, CA).

Plasmids were combined with the cationic lipid-shelled microbubbles by electrostatic charge coupling (Fig. 1) as previously demonstrated in (Christiansen et al. 2003;Phillips et al. 2010) and coupling efficiency was assessed over a range of plasmid concentrations. Initially, a calibration curve for plasmids (CMV-pKred) diluted in PBS at concentrations of 0 (PBS alone), 3.13, 6.25, and 12.5 μg/ml was determined by spectroscopy at 260nm. Optical density of the CMV-pKred plasmid solution increased linearly ($R^2 = 0.999$) with increasing concentration of DNA over the range between 0 and 12.5 μg/ml. This range covered the plasmid/microbubble concentrations examined and exceeded those used in experiments.

A combination of 0, 5, 10 or 20 μg of the plasmid and 5×10^8 microbubbles were diluted in 1.6 ml of PBS and incubated for 15 minutes during which time it was gently mixed. After incubation the dispersion was centrifuged for 4 minutes at 1000G. Non-adherent plasmids were separated from microbubbles through centrifugal flotation. The eluent was collected and plasmid concentration assessed by optical density measurement at 260 nm on a Beckman DU-640 spectrophotometer (Beckman Coulter, Brea, CA). Optical density measurements of the eluents from plain microbubbles (not coupled with any plasmid DNA) were negligible. This result indicates that the lipids alone did not interfere with absorbance readings, nor was turbidity present in the samples. The plasmid DNA calibration curve was compared to the absorbance of the non-conjugated plasmids in the microbubble eluents. The amount of plasmid coupled to the microbubbles was calculated as the total amount of plasmid added to the initial mixture minus the portion in the eluent. The plasmid to microbubble ratio for experiments was maintained at 1μg DNA/5×10^6 microbubbles. Maximal electrostatic coupling of bubbles and plasmids was achieved by gentle mixing and incubating for 15 minutes prior to use.

In Vitro Gene Delivery

Ultrasound triggered plasmid DNA delivery from microbubbles was examined *in vitro* using a visual assay of gene transfection via red fluorescent protein (RFP) expression. 24 hours after cells had been plated, the media in each Opticell was replaced with fresh media containing one of the following three combinations of reagents: microbubbles (1.5×10^8) coupled with 30 μg of the CMV-RFP plasmid (final solution in each Opticell - 3 μg/ml), 30 μg CMV-RFP plasmid alone (no microbubbles), or equivalent volume of pure saline (no plasmid or microbubbles).

The insonation apparatus, as seen in Fig. 2, included the use of a single-element, focused 1 MHz transducer (Panametrics, Waltham, MA) and an ESP300 motion controller linear stage (Newport Research Corp., Irvine, CA) to precisely position it. Pulse lengths and peak pressures were varied while the pulse repetition frequencies, were chosen to maintain a constant duty cycle of 0.5% (Table 1). The pulses were generated by using the combination of an AWG2021 arbitrary waveform generator (Tektronix, Beaverton, OR), a 5077PR pulser/receiver (Panametrics, Waltham, MA) and a 60 dB power amplifier (model A-500, ENI, Rochester, NY). The resulting peak negative pressure (PNP), and beam profiles produced by the Panametrics transducer were measured using a calibrated hydrophone (GL-0200, Onda Corp., Sunnyvale, CA) prior to experimentation. For each amplitude and waveform, these

measurements were collected across the center of the beam at a range of 28mm - corresponding to the transmit voltage functions and range used in the experiments (Fig. 3).

Each Opticell was immersed in a water bath held at 37°C using a recirculating heater (Model 73A0A11B, Polyscience, Niles, IL). Prior to insonation a two minute wait period in the water tank allowed time for the bubbles to rise toward the cells. The submerged transducer was placed 18mm above the surface of the Opticell. A neoprene absorber was placed below and angled at 30 degrees to prevent standing wave formation (Fig. 2). The motion controller translated the transducer across the Opticells in order to apply ultrasound to the 0.8cm × 6cm areas of cell growth. The −6dB beamwidth and translation speed determined the time during which each point in the Opticell was insonated. At a translation speed of 2.0mm/s and beamdwidth of 10mm every cell was insonated for approximately 5 seconds. Each Opticell contained two non-overlapping insonation regions (0.8cm × 6cm) and one control region of the same size not exposed to ultrasound. Following insonation, Opticells were immediately flushed with phosphate buffered saline (PBS) and replenished with fresh serum-containing growth media. Gene transfection efficacy was measured 24 hours after treatment as the number of fluorescent cells per region and then normalized to the total number of cells per unit area. Using both phase contrast and fluorescence microscopy, all fluorescent cells within the region of insonation were counted along with the total number of cells present. Two Opticells were used per treatment group and the experiment was repeated at least twice on separate days.

Clinical ultrasound comparison

As a proof-of-principle, ultrasound mediated gene delivery from a clinical ultrasound scanner was investigated both *in vitro* and *in vivo*. The microbubble gene delivery system was implemented with a 15L8 linear array transducer in conjunction with a Sequoia 512 imaging system (Siemens Medical Solutions). Using the Contrast Pulse Sequence (CPS) (Phillips 2001) contrast specific imaging mode the probe was programmed to emit pulses for one second every two seconds for a total of 1 minute at a burst mechanical index (BMI) of 1.8. Pulses, as measured using the aforementioned hydrophone, were centered at 5 MHz, 5 cycles in length and emitted at a PRF of 5 kHz with a peak negative pressure of 1.6 MPa at 1.0 cm from the probe (equivalent to the distance between the probe and the Opticell *in vitro* or rat carotid *in vivo*). The single element Panametrics transducer was programmed to emit 1MHz Gaussian pulses at an equivalent duty cycle, but lower peak negative pressure (600 kPa). Although cavitation is dependent on pulse amplitude and frequency, user control over frequency, pressure amplitude, and PRF in "burst mode" were not feasible with the clinical system. Instead, we matched the duty cycle and chose a peak pressure of 600 kPa which more closely matched the time-averaged intensity. All other cell, microbubble, and experimental conditions were kept constant as compared to the prior *in vitro* studies.

Statistical Analysis

Statistical significance for all control studies was determined with two-sided student's t-tests. Analysis of variance (ANOVA) was used to determine statistical significance between groups. A p-value less than 0.05 was considered significant.

Results

Microbubble and Plasmid Conjugation

Following centrifugal flotation the Coulter-counted average bubble diameter was determined to be 2.4 μm. The coupling capacity of the cationic microbubbles was measured via assessment through optical density analysis of non-coupled plasmid DNA (Fig. 4A). Saturation of these bubbles occurred at a concentration of 5μg DNA/5×10^8 microbubbles. As presented in Fig. 4B, 95% of the plasmid DNA was adherent to the cationic microbubbles at a concentration of

5μg/half billion bubbles. Beyond saturation excess plasmid was collected in the eluent (Fig. 4B). The optimal ratio for use in experiments was selected as the saturation concentration. Saturation corresponds to ~2500 plasmids per bubble or 200 plasmids per μm^2 of surface area. Surface area was calculated based on the bubble size distribution determined by the Coulter counter. Cationic microbubbles were selected because they were shown to enhance coupling of plasmid DNA (Unger et al. 1997) and will likely offer an advantage *in vivo*.

In Vitro Gene Delivery

Both gene transfection efficacy and cell viability were investigated for the range of ultrasound parameters tested. Successful gene transfection was indicated by the presence of red fluorescent protein expression in the smooth muscle cells (Fig. 5). Gene delivery was measured as the percentage of transfected cells in each insonated (500 kPa, 50 cycles per pulse, 100 Hz PRF) or control region of each Opticell. Without ultrasound very few if any smooth muscle cells were transfected, as seen in the example fluorescence image in Fig. 5a and quantitatively in Fig. 6a. Smooth muscle cells treated with fresh media only, fresh media with microbubbles, fresh media with plasmid DNA, or fresh media with plasmid-coupled microbubbles resulted in no significant transfection (Fig. 6a) or change in cell viability (Fig. 6b) without the presence of ultrasound. Cells in each of these control groups proliferated equally, exhibited equivalent viability before and after treatment, and expressed little (≤0.01% cells transfected) or no red fluorescent protein. Viability was significantly reduced (p = 0.018) in both groups treated with microbubbles and ultrasound regardless of whether DNA was present (53 +/− 27%) or not (19 +/− 8%). Ultrasound alone did not significantly affect transfection or viability. Upon addition of 1 MHz, 50 cycle ultrasound exposure the number of adherent and viable cells decreased with increasing peak negative acoustic pressure as shown qualitatively in Fig. 7 and quantitatively in Fig. 8b. Gene transfection increased with increasing acoustic peak negative pressure (Fig. 8a) up to approximately 0.87% at 300 kPa, beyond which transfection rates slowly declined up to the maximum evaluated pressure, 950 kPa. Student's t-tests confirmed the statistically significance of this peak at 300 kPa from pressures at or below 200 kPa and at or above 500 kPa. The corresponding viability of cells at 300 kPa was only 24%. Statistical analysis of variance (ANOVA) revealed that the relationships between both transfection and viability with peak negative pressure were statistically significant (p < 0.001).

Pulse length, as defined by the number of continuous cycles per pulse was then evaluated at a constant peak negative acoustic pressure of 300 kPa. Gene transfection increased with increasing cycle number up to 50 cycles per pulse (0.87 +/− 0.26%), beyond which no further increase in gene transfection was observed (Fig. 9a). The viability of these cells did not significantly differ over the range of pulse lengths evaluated with the exception of 1 cycle per pulse (p = 0.047, Fig. 9b). Under single cycle pulses of ultrasound at 300 kPa approximately 54.7 +/− 11.7% of cells remained attached and viable whereas only 23.4 +/− 14.4% remained viable under exposure to 100 cycle pulses. The relationships between both transfection and viability with pulse length were statistically significant by ANOVA (p = 0.003 and 0.012 respectively).

Clinical-ultrasound-induced gene transfection

Transcutaneous clinical ultrasound conditions were sufficient to mediate delivery of plasmid DNA from microbubble carriers to the smooth muscle cells. Applied *in vitro,* the contrast pulse burst mode of the 15L8 linear array resulted in similar transfection rates (38.0 +/− 3.6 cells/ cm^2) as compared to the single element transducer (50.5 +/− 16.2 cells/cm^2). Although the ultrasound pressure and frequency were different, the results were not statistically different (Fig. 10a). Both systems are capable of enhancing gene transfection.

Discussion

Gene transfection through ultrasound-mediated delivery of naked plasmid DNA from microbubbles has been performed in the past by others, however the studies at hand sought to investigate the use of positively charged microbubbles and ultrasound conditions necessary for gene transfection to vascular smooth muscle cells. We found that relatively low pressures (200–400 kPa) and longer pulse lengths increased cell viability while also increasing gene transfection.

Microbubble coupling comparison

We achieved 95% coupling of the plasmid DNA to the cationic microbubbles. This efficiency was observed at a concentration of $5\mu g/0.5 \times 10^9$ bubbles and was found to also be the saturation concentration. The saturation concentration determined by the Christiansen (Christiansen et al. 2003) group is comparable although a different plasmid was used in those experiments. The charge of the microbubbles should be taken into account when selecting an agent for gene delivery which is why we chose to use cationic microbubbles for the remainder of our experiments. The enhanced coupling capacity of the positive microbubbles may not significantly affect transfection in the static *in vitro* setting. However, cationic microbubbles may serve to enhance gene delivery inside a vessel lumen under blood flow *in vivo* where non-adherent plasmids may never reach the vessel wall without the help of a microbubble carrier. Furthermore, it has been suggested that by attaching the DNA to cationic lipids the plasmids are better protected from endonucleases and hepatic uptake (Ruysschaert et al. 1994).

Gene transfection

The results of the studies herein demonstrated a dependency of both pulse length and amplitude on transfection rate. The optimal acoustic pressure for gene transfection to the vascular smooth muscle cells was determined to be 300 kPa – a pressure significantly high enough to induce lipid shelled microbubble rupture (Chomas et al. 1999; Dayton et al. 1999; Shi et al. 2006; Shin-Yuan et al. 2006). Longer pulses resulted in greater transfection although little difference in transfection rates was observed beyond 10 cycle pulses. This result may be a consequence of the rupture of intact microbubbles after only several cycles of ultrasound. Longer pulse durations at lower pressures and frequencies were not investigated in this study. It is possible that lower pressures and longer pulse durations could also enhance gene transfection while maintaining higher viability rates. The thresholds for cavitation, which we know are highly dependent on frequency and pressure amplitude, may not be equivalent to those for gene transfection. We observed comparable transfection rates when using the clinical (5 MHz) system and the single element (1 MHz) transducers even though the pressure amplitudes and frequencies were not matched. It was not necessary to fully match the ultrasound parameters in order to achieve equivalent levels of gene transfection from each transducer.

The studies performed by the authors herein applied comparable ultrasound conditions as compared to others who have performed microbubble mediated gene delivery studies and have achieved similar transfection efficiencies. Currently we are able to achieve approximately 1% transfection *in vitro* under our current protocol, which is consistent with the observations (1–5% transfection efficiencies) of others using similar microbubble-gene delivery techniques (Miller et al. 2003; Rahim et al. 2006a; Rahim et al. 2006b; Meijering et al. 2007). For instance, Rahim and Porter (Rahim et al. 2006a) also applied 1 MHz ultrasound at a PRF of 1 kHz and achieved transfection rates in Chinese Hamster Ovary cells around 1–5%. Similarly, in a study by Miller, et al. (Miller et al. 2003) a 1.5 MHz scanner operating at acoustic pressures between 0.7 to 2.3 MPa was used to transfect 1–5% of epidermoid cells. Both of these studies were conducted in Opticell chambers as well. One group studying ultrasound-microbubble delivery to cancer cells noted a 16% gene delivery efficiency in one type of cancer cell line (Hela), but

a 31-fold lower transfection rate (>1%) in other non-cancerous cell lines (Feril et al. 2006). The differences in transfection efficacies is likely to be at least partially due to the difference in cell type and experimental set up and is discussed later. The Porter group also found that acoustic pressure, microbubble concentration and PRF affected both gene delivery and cell viability (Rahim et al. 2006a). The optimal microbubble concentration as found by this group (200×10^6/ml) is comparable to our selected concentration of 150×10^6/ml. Although microbubble concentration was not varied in the present study, prior experiments with much greater or lower concentrations of microbubbles were not as successful (data not shown).

Viability

Both gene transfection efficiency and cell viability are related to the acoustic pressure and pulse length as seen in Figs. 9 and 10 respectively. We found the optimal acoustic pressure for gene transfection to vascular smooth muscle cells to be 300 kPa beyond which gene transfection decreased. The viability of these cells was greatly reduced down to less than 50% at intensities greater than or equal to 300 kPa. In other studies applying 0.5–1.5 MHz ultrasound (Guzman et al. 2001a;Miller et al. 2003;Zarnitsyn and Prausnitz 2004;Feril et al. 2006;Rahim et al. 2006a;Rahim et al. 2006b;Meijering et al. 2007;Karshafian et al. 2009) the peak pressure required to reduce cell viability below 90% varies considerably from 0.22 MPa (Rahim et al. 2006b) to approximately 1 MPa (Guzman et al. 2001a), and is likely due to differences in cell type and acoustic pulsing parameters. Not all studies measured viability in the same way. Some studies measured viability as the percent of cells which did not uptake propidium iodide (Zarnitsyn and Prausnitz 2004;Karshafian et al. 2009) whereas we defined it as the percent difference in cell density as compared to control cells which were not insonated. It is probable that smooth muscle cells do not adhere to Opticell membranes as well as other cell lines and therefore many were "knocked off" during insonation rather than dying as was observed by Lawrie et al (2000). A consequence of this "knocking off", and other differences in an *in vitro* experiment, is that these experiments may overestimate the cell loss actually anticipated *in vivo* where cells are firmly bound in a natural environment.

Comparison of experimental designs

One of the main differences between prior studies and our studies is the cell type used. We investigated vascular smooth muscle cells because of their critical role in clinical restenosis. Secondly, our *in vitro* experimental set up, we strove to minimize side effects which may have been caused by plating apparatus, lack of flow, and cellular state. In experiments by others, who plated cells on hard plastic culture dishes or well plates (Feril et al. 2006; Tsai et al. 2009), standing waves may have occurred. Standing waves can result in higher pressures than would otherwise be observed *in vivo*. Similarly, some groups examined sonoporation (Karshafian et al. 2009) or gene transfection (Guzman et al. 2001a; Guzman et al. 2001b) on cells in solution. Although these studies provide information about acoustic optimization for *in vitro* sonoporation of some cell types, they do not closely approximate *in vivo* conditions of cells in tissue. Cells in tissues are adherent to each other and are affected by their neighboring cells. In fact, a study by Kinoshita and Hynynen (2007) revealed that standing wave formation and the method of cell culture greatly affect sonoporation and viability of cells. We performed all *in vitro* experiments in acoustically transparent Opticell chambers to eliminate standing wave formation and more closely approximate the *in vivo* environment. Other groups have exposed cells to lipofecting agents during insonation, or exposed the cells to plasmid DNA for long periods of time (hours to days) (Feril et al. 2006; Rahim et al. 2006a; Rahim et al. 2006b; Meijering et al. 2007). Although these techniques enhance gene transfection they are not realistic for *in vivo* settings since lipofecting agents are too potent and plasmid DNA would be cleared from the circulation within minutes. In our experiments, microbubbles and plasmids were only exposed to the cells for ~7 minutes. By coupling our plasmid DNA to the

microbubbles we believe the circulation time and probability of reaching the vessel wall (via ultrasound radiation force) will both be enhanced *in vivo*.

Preliminary clinical ultrasound delivery to balloon angioplasty model in vivo

For comparison the same CPS mode pulsing scheme was employed in a rat carotid model of balloon angioplasty. All animal experiments were conducted under University of Virginia Animal Care and Use Committee (ACUC) approved protocols. A 2F Fogarty balloon catheter was introduced through an arteriotomy and advanced to the left common carotid of a Sprague-Dawley rat. Once in the common carotid, the balloon was inflated with 0.2 ml of saline and drawn back towards the inflation device. This process was repeated 3 times and effectively removed the endothelium from the common carotid (Clowes et al. 1983). Three days following balloon angioplasty the left carotid artery was located non-invasively using ultrasound imaging prior to bubble injection. With the 15L8 transducer parallel to the artery a mixture of the plasmid coupled microbubbles (400ng/million bubbles) was infused into the cannulated right jugular vein at a rate of 2×10^7 microbubbles/min for a total of 5 minutes. Ultrasound was applied in CPS burst mode to the injured left carotid during the same 5 minutes. The right carotid, through which microbubbles also flowed, but which was not insonated, served as a treatment control. Three days after microbubble-plasmid delivery, the animal was euthanized and left and right carotids were processed for frozen histological cross sectioning.

Transverse cross sections (6μm thick) of the injured carotid and contralateral right carotid (control) were imaged using a confocal microscope (FluoView, Olympus America Inc., Center Valley, PA). Nuclei were stained blue with DAPI. Elastic lamina were identified by exciting the tissue at 488 nm resulting in autofluorescent green emission. Successful plasmid DNA transfection and expression were indicated by red fluorescent protein (RFP) excitation at 550nm. RFP was present in at least the first layer of smooth muscle cells indicating successful localized gene delivery (Fig. 10C). The lack of nuclei lining the outside of the innermost layer of elastic lamina indicates the successful removal of the endothelium in the injured vessel, whereas the nuclei were still present in the lumen of the contralateral control vessel (Figs. 10B, 10C).

We have demonstrated that *in vitro* and *in vivo* gene transfection can be localized to the area of insonation and that microbubbles are required in order to achieve significant transfection. The contrast burst mode pulsing scheme of the linear array ultrasound system, as applied to the cells both *in vitro* and to the injured carotid artery *in vivo*, resulted in significant gene transfection of smooth muscle cells compared to non-insonated controls. Low ultrasound frequencies (0.02–2.5 MHz) are usually selected for bursting bubbles and transferring genes into cells, but we observed similar *in vitro* transfection rates with the linear array at ~5 MHz, (peak negative pressure ~1.6 MPa, MI = 1.9), and the single element transducer at 1 MHz (peak negative pressure = 0.6 MPa, MI estimated as 0.6). Thus, our results suggest the potential to tightly integrate an imaging system with a therapeutic system. This is an important practical consideration since image guidance is highly desirable in any transcutaneous procedure.

Prior studies by our group have shown that intravascular ultrasound is capable of localizing gene transfection to porcine coronary arteries following angioplasty (Phillips et al. 2010). Gene delivery to a vessel wall using ultrasound and microbubbles has previously been demonstrated in surgically ligated vessels (Taniyama et al. 2002). Our transcutaneous method of ultrasound application was completely non-invasive. Occlusion of blood flow in the injured vessel during the period of insonation was not necessary in order to achieve localized transfection. Although some of the ultrasound parameters may need to be altered for use in humans or other species our ultrasound mediated gene delivery system is non-invasive except for the IV injection of bubbles in saline. Future experiments are required to investigate the acoustic intensity threshold beyond which tissue damage occurs. Although additional control experiments are needed in

order to fully understand the parameters necessary for *in vivo* delivery we have shown that it is possible to localize gene transfection with clinical transthoracic ultrasound.

Conclusions

Cationic microbubbles served as plasmid DNA carriers and are up to 44% more efficient at coupling DNA which may increase their ability to deliver a payload *in vivo*. No significant gene transfection occurred when microbubbles, plasmid DNA, or a combination of both were incubated with cells. Similarly, no combination of plasmid DNA and microbubbles had an effect on viability of the cells. Only in the presence of ultrasound did gene transfection occur. The transfected cells were localized to the region of insonation within Opticells. Gene delivery to smooth muscle cells was enhanced when low acoustic pressures around 300 kPa were employed at pulses at least 10 cycles in length. The observed transfection rates (~1%) in this study are comparable to rates observed by other groups, however gene delivery to smooth muscle cells has not previously been reported using our system of ultrasound mediated microbubble delivery.

Our combined *in vitro* and *in vivo* results suggest that gene delivery to smooth muscle cells in injured vessels following angioplasty may have applications for localized therapy. The proof of principle study is the first, to our knowledge, to demonstrate successful *in vivo* plasmid DNA delivery to carotid artery smooth muscle cells following acute angioplasty via transcutaneous ultrasound with cationic lipid microbubbles. Addition of therapeutically active genes instead of RFP may serve as anti-proliferative agents for the treatment of restenosis.

Acknowledgments

References

Anwer K, Kao G, Proctor B, Anscombe I, Florack V, Earls R, Wilson E, McCreery T, Unger E, Rolland A, Sullivan SM. Ultrasound enhancement of cationic lipid-mediated gene transfer to primary tumors following systemic administration. Gene Therapy 2000;7:1833–1839. [PubMed: 11110415]

Byrne RA, Sarafoff N, Kastrati A, Schömig A. Drug-Eluting Stents in Percutaneous Coronary Intervention: A Benefit-Risk Assessment. Drug Safety 2009;32:749–770. [PubMed: 19670915]

Camenzind E, Steg PG, Wijns W. Stent thrombosis late after implantation of first-generation drug-eluting stents - A cause for concern. Circulation 2007;115:1440–1455. [PubMed: 17344324]

Christiansen JP, French BA, Klibanov AL, Kaul S, Lindner JR. Targeted tissue transfection with ultrasound destruction of plasmid-bearing cationic microbubbles. Ultrasound in Medicine and Biology 2003;29:1759–1767. [PubMed: 14698343]

Clowes AW, Reidy MA, Clowes MM. Mechanisms of stenosis after arterial injury. Laboratory Investigation 1983;49:208–215. [PubMed: 6876748]

Dayton PA, Morgan KE, Klibanov AL, Brandenburger GH, Ferrara KW. Optical and acoustical observations of the effects of ultrasound on contrast agents. Ieee Transactions on Ultrasonics Ferroelectrics and Frequency Control 1999;46:220–232.

Duvshani-Eshet M, Baruch L, Kesselman E, Shimoni E, Machluf M. Therapeutic ultrasound-mediated DNA to cell and nucleus: bioeffects revealed by confocal and atomic force microscopy. Gene Therapy 2006;13:163–172. [PubMed: 16177822]

Eisenstein EL, Anstrom KJ, Kong DF, Shaw LK, Tuttle RH, Mark DB, Kramer JM, Harrington RA, Matchar DB, Kandzari DE, Peterson ED, Schulman KA, Califf RM. Clopidogrel Use and Long-term Clinical Outcomes After Drug-Eluting Stent Implantation. JAMA 2007;297:159–168. [PubMed: 17148711]

Feril LB, Ogawa R, Tachibana K, Kondo T. Optimized ultrasound-mediated gene transfection in cancer cells. Cancer Science 2006;97:1111–1114. [PubMed: 16925580]

Ferrara K, Pollard R, Bordeni M. Ultrasound microbubble contrast agents: Fundamentals and application to gene and drug delivery. Annual Review of Biomedical Engineering 2007;9:415–447.

Greenleaf WJ, Bolander ME, Sarkar G, Goldring MB, Greenleaf JF. Artificial cavitation nuclei significantly enhance acoustically induced cell transfection. Ultrasound in Medicine and Biology 1998;24:587–595. [PubMed: 9651968]

Guzman HR, Nguyen DX, Khan S, Prausnitz MR. Ultrasound-mediated disruption of cell membranes. I. Quantification of molecular uptake and cell viability. Journal of the Acoustical Society of America 2001a;110:588–596. [PubMed: 11508983]

Guzman HR, Nguyen DX, Khan S, Prausnitz MR. Ultrasound-mediated disruption of cell membranes. II. Heterogeneous effects on cells. Journal of the Acoustical Society of America 2001b;110:597–606. [PubMed: 11508985]

Karshafian R, Bevan PD, Williams R, Samac S, Burns PN. Sonoporation by ultrasound-activated microbubble contrast agents: effect of acoustic exposure parameters on cell membrane permeability and cell viability. Ultrasound in Medicine and Biology 2009;35:847–860. [PubMed: 19110370]

Kim HJ, Greenleaf JF, Kinnick RR, Bronk JT, Bolander ME. Ultrasound-mediated transfection of mammalian cells. Human Gene Therapy 1996;7:1339–1346. [PubMed: 8818721]

Kinoshita M, Hynynen K. Key factors that affect sonoporation efficiency in in vitro settings: The importance of standing wave in sonoporation. Biochemical and Biophysical Research Communications 2007;359:860–865. [PubMed: 17568561]

Lawrie A, Brisken AF, Francis SE, Cumberland DC, Crossman DC, Newman CM. Microbubble-enhanced ultrasound for vascular gene delivery. Gene Therapy 2000;7:2023–2027. [PubMed: 11175314]

Mayer CR, Bekeredjian R. Ultrasonic gene and drug delivery to the cardiovascular system. Advanced Drug Delivery Reviews 2008;60:1177–1192. [PubMed: 18474407]

Meijering BDM, Henning RH, Van Gilst WH, Gavrilovic I, Van Wamel A, Deelman LE. Optimization of ultrasound and microbubbles targeted gene delivery to cultured primary endothelial cells. Journal of Drug Targeting 2007;15:664–671. [PubMed: 18041634]

Meijering BDM, Juffermans LJM, van Wamel A, Henning RH, Zuhorn IS, Emmer M, Versteilen AMG, Paulus WJ, van Gilst WH, Kooiman K, de Jong N, Musters RJP, Deelman LE, Kamp O. Ultrasound and Microbubble-Targeted Delivery of Macromolecules Is Regulated by Induction of Endocytosis and Pore Formation. Circulation Research 2009;104:679–U226. [PubMed: 19168443]

Miller DL, Dou CY, Song JM. DNA transfer and cell killing in epidermoid cells by diagnostic ultrasound activation of contrast agent gas bodies in vitro. Ultrasound in Medicine and Biology 2003;29:601–607. [PubMed: 12749930]

Orr AW, Lee MY, Lemmon JA, Yurdagul A Jr, Gomez MF, Schoppee Bortz PD, Wamhoff BR. Molecular Mechanisms of Collagen Isotype-Specific Modulation of Smooth Muscle Cell Phenotype. Arteriosclerosis, Thrombosis, and Vascular Biology. 2008 ATVBAHA.

Owens GK, Kumar MS, Wamhoff BR. Molecular regulation of vascular smooth muscle cell differentiation in development and disease. Physiological Reviews 2004;84:767–801. [PubMed: 15269336]

Phillips LC, Klibanov AL, Bowles DK, Ragosta M, Hossack JA, Wamhoff BR. Focused in vivo Delivery of Plasmid DNA to the Porcine Vascular Wall via Intravascular Ultrasound Destruction of Microbubbles. Journal of Vascular Research 2010;47:270–274. [PubMed: 19923850]

Rahim A, Taylor SL, Bush NL, Ter Haar GR, Bamber JC, Porter CD. Physical parameters affecting ultrasound/microbubble-mediated gene delivery efficiency in vitro. Ultrasound in Medicine and Biology 2006a;32:1269–1279. [PubMed: 16875960]

Rahim AA, Taylor SL, Bush NL, ter Haar GR, Bamber JC, Porter CD. Spatial and acoustic pressure dependence of microbubble-mediated gene delivery targeted using focused ultrasound. Journal of Gene Medicine 2006b;8:1347–1357. [PubMed: 16981246]

Ren JL, Wang ZG, Zhang Y, Zheng YY, Li XS, Zhang QX, Wang ZX, Xu CS. Transfection efficiency of TDL compound in Huvec enhanced by ultrasound-targeted microbubble destruction. Ultrasound in Medicine and Biology 2008;34:1857–1867. [PubMed: 18524464]

Ruysschaert JM, Elouahabi A, Willeaume V, Huez G, Fuks R, Vandenbranden M, Distefano P. A novel cationic ampiphile for transfection of mammalian-cells. Biochemical and Biophysical Research Communications 1994;203:1622–1628. [PubMed: 7945312]

Shi WT, Forsberg F, Vaidyanathan P, Tornes A, Ostensen J, Goldberg BB. The influence of acoustic transmit parameters on the destruction of contrast microbubbles in vitro. Physics in Medicine and Biology 2006;51:4031–4045. [PubMed: 16885622]

Taniyama Y, Tachibana K, Hiraoka K, Namba T, Yamasaki K, Hashiya N, Aoki M, Ogihara T, Yasufumi K, Morishita R. Local delivery of plasmid DNA into rat carotid artery using ultrasound. Circulation 2002;105:1233–1239. [PubMed: 11889019]

Tsai KC, Fang SY, Yang SJ, Shieh MJ, Lin WL, Chen WS. Time dependency of ultrasound-facilitated gene transfection. Journal of Gene Medicine 2009;11:729–736. [PubMed: 19455570]

Unger EC, Hersh E, Vannan M, Matsunaga TO, McCreery M. Local drug and gene delivery through microbubbles. Progress in Cardiovascular Diseases 2001;44:45–54. [PubMed: 11533926]

Unger EC, McCreery TP, Sweitzer RH. Ultrasound enhances gene expression of liposomal transfection. Investigative Radiology 1997;32:723–727. [PubMed: 9406011]

Unger EC, Porter T, Culp W, Labell R, Matsunaga T, Zutshi R. Therapeutic applications of lipid-coated microbubbles. Advanced Drug Delivery Reviews 2004;56:1291–1314. [PubMed: 15109770]

Wu JR, Ross JP, Chiu JF. Reparable sonoporation generated by microstreaming. Journal of the Acoustical Society of America 2002;111:1460–1464. [PubMed: 11931323]

Zarnitsyn VG, Prausnitz MR. Physical parameters influencing optimization of ultrasound-mediated DNA transfection. Ultrasound in Medicine and Biology 2004;30:527–538. [PubMed: 15121255]
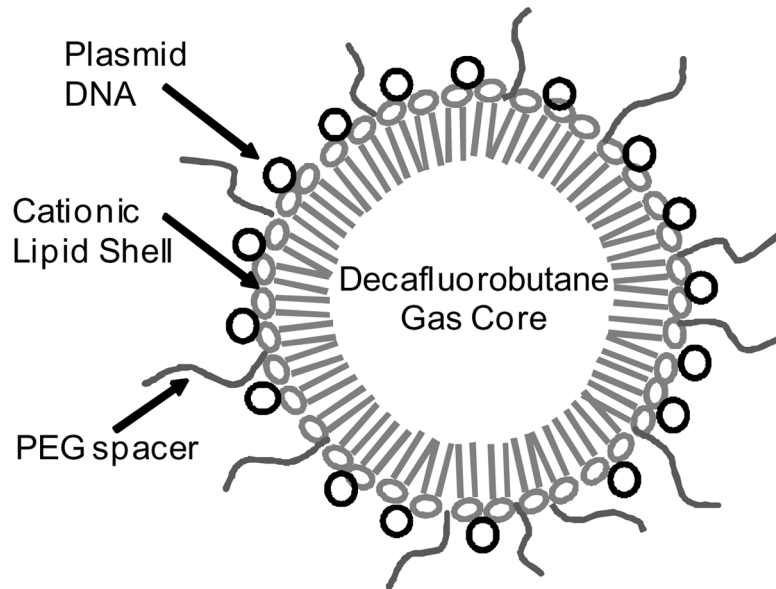
Figure 1.
Schematic diagram of microbubbles. Negatively charged plasmid DNA encoding red fluorescent protein (CMV-RFP) was conjugated to cationic microbubbles through electrostatic binding. Polyethylene glycol (PEG) spacers were added to enhance longevity *in vivo*.
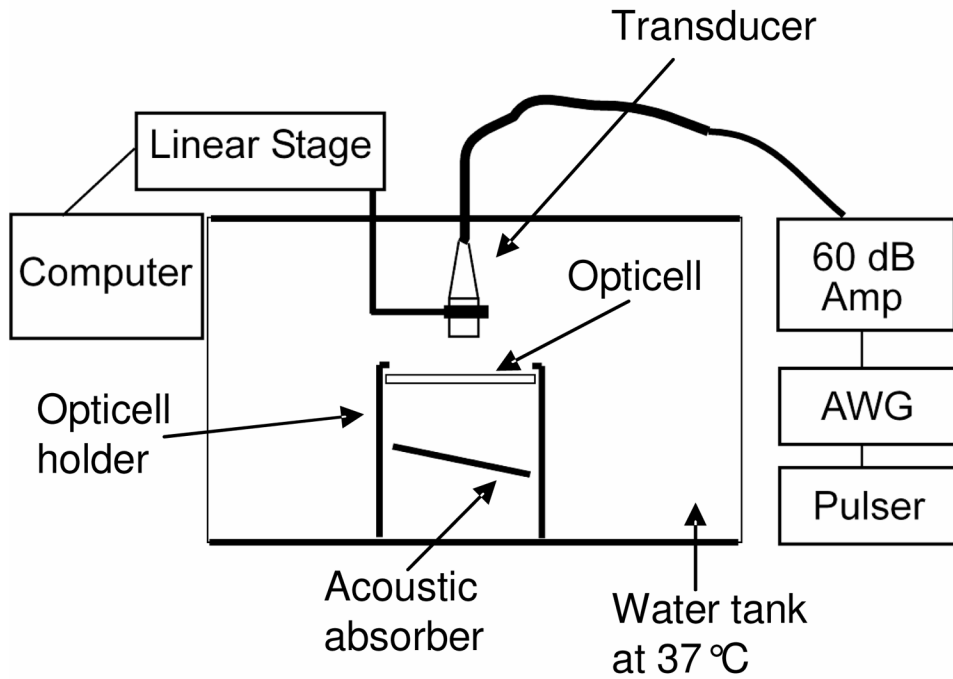
Figure 2.
In vitro experiments were performed in a water tank at 37°C. The transducer was oriented directly above the cells and its position was controlled with a linear motion controller. An acoustic neoprene absorber (7mm thick) below the Opticell was angled at 30 degrees to prevent standing wave formation. The PRF and pulse duration were set using a pulser and arbitrary waveform generator respectively. All pulses were amplified with a 60dB amplifier before reaching the transducer.
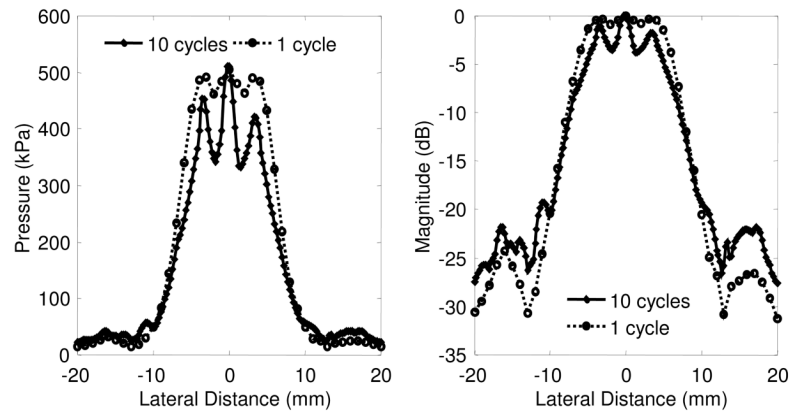
Figure 3.
Acoustic pressure profile of the V302 transducer operating at 1MHz with either a 10 cycle pulse (solid line) or 1 cycle pulse (dotted line). Acoustic pressures, as measured by a PVDF hydrophone, were collected at a distance 18mm from the face of the transducer which is equivalent to 23 mm from the axial focal distance. The beam profile is displayed in both peak pressure (left) and magnitude in decibels (right).
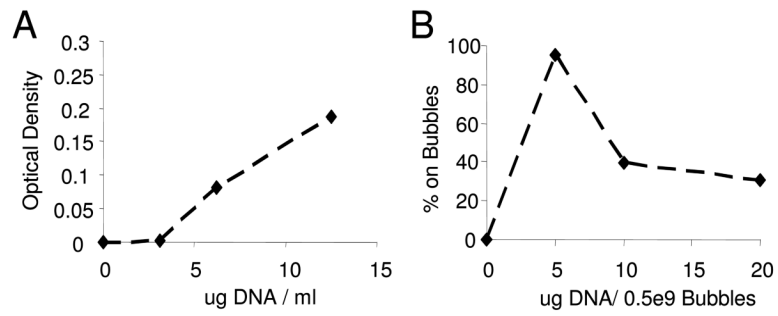
Figure 4.
A) Positively charged microbubbles were incubated with a range of concentrations of plasmid DNA. Centrifugal flotation of plasmid-coupled microbubbles was performed to separate non-coupled plasmids from the microbubbles. A) Optical densities of the non-coupled plasmids were measured from the eluents. B) Based on the amount of plasmid recovered the percentage of the DNA coupled to the microbubbles was calculated. Saturation occured with 5ug of DNA/ 5×10^8 bubbles.
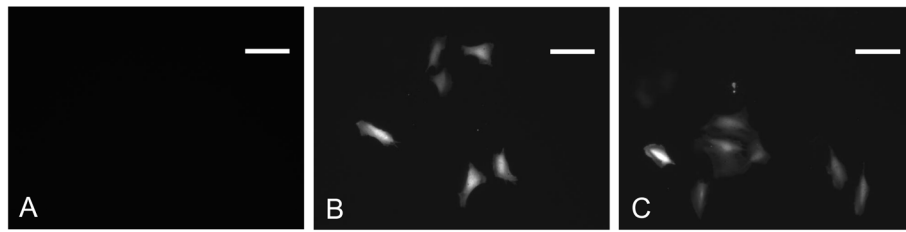
Figure 5.
Example fluorescent images of transfected smooth muscle cells exposed to CMV-RFP coupled microbubbles A) without ultrasound and B) with 50 cycle, 300 PNP or C) 20 cycle 500 PNP ultrasound exposure. Fluorescence microscopy was performed 24 hours after insonation. By exciting cells at 512 nm the red fluorescent protein was visualized. No expression was observed in cells which were not exposed to ultrasound. *scalebar = 100 μm.
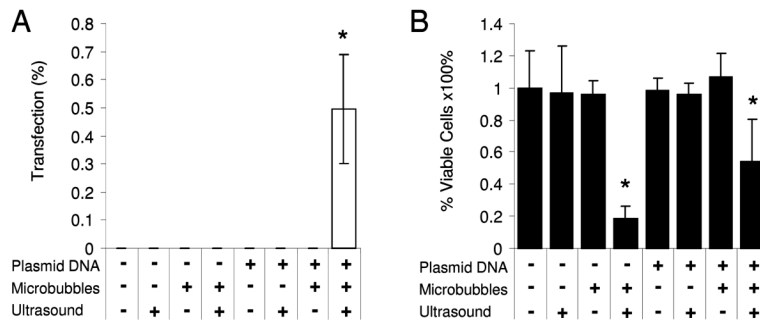
Figure 6.
Significant gene transfection occurs only with the combination of ultrasound, microbubbles, and DNA. Gene transfection efficacy (A) and cell viability (B) were assessed following treatment with combinations of fresh media only (left-most combination), microbubbles, plasmid DNA, or plasmid-coupled microbubbles in the absence of ultrasound and presence of ultrasound (500 kPa, 50 cycles, PRF = 100 Hz). Only the combination of microbubbles with ultrasound reduced viability. (n≥4, results expressed as mean +/− S.D., * indicates $p < 0.05$)
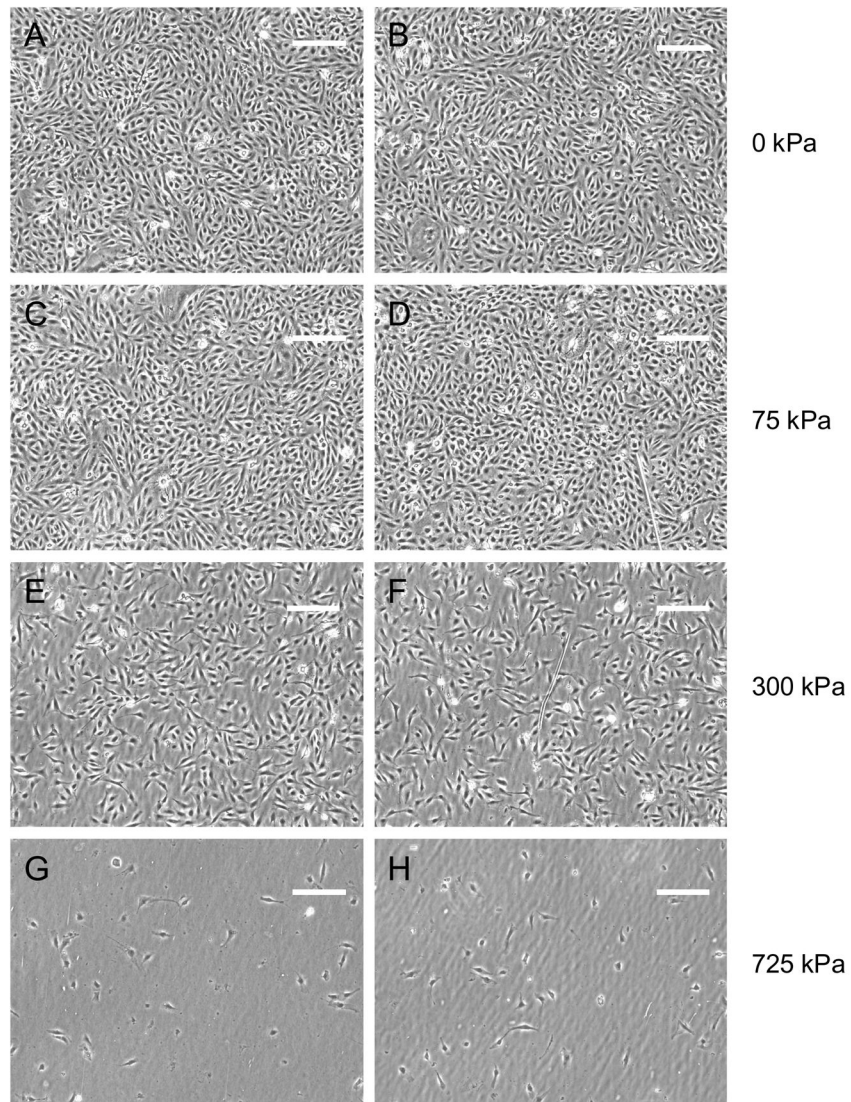
Figure 7.
Brightfield images of smooth muscle cells at 24 hours post-insonation with plasmid-bearing microbubbles. Left and right columns are from separate cell dishes and the applied peak negative pressures are listed to the right of the images. Scalebar = 250 µm.
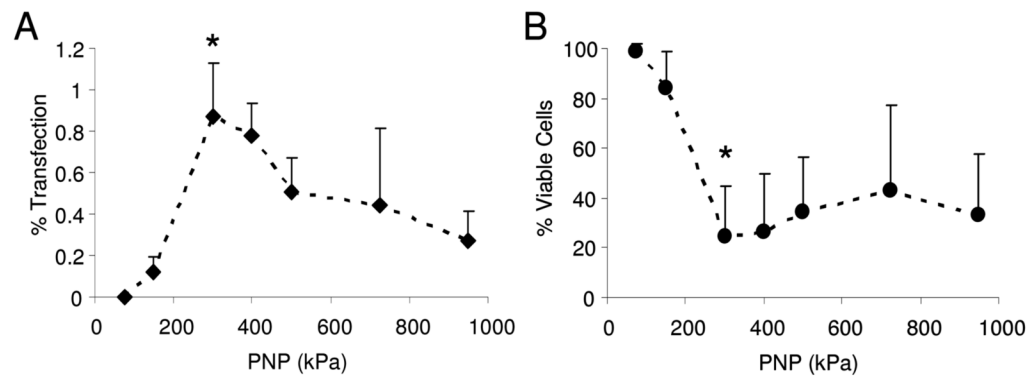
Figure 8.
Transfection efficacy (% of the cells transfected) and viability (those alive and adherent to the membrane) were measured following insonation with a 1 MHz pulse of 50 cycles at a PRF of 100 Hz while peak negative pressure was ramped from 0 to 950 kPa. Transfection efficacy was calculated as the percentage of fluorescent cells out of the total number of cells. Viability was calculated as the ratio of cell densities between cells treated with ultrasound and without ultrasound. Maximal transfection (0.87%) occurred at 300 kPa and corresponded to 24% viability (n=≥4, results expressed as mean +/− S.D., * indicates $p < 0.05$).
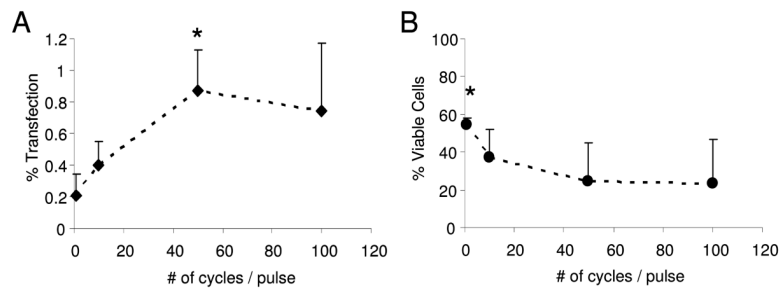
Figure 9.
Transfection efficacy (% of the cells transfected) and viability (those alive and adherent to the membrane) were measured as a function of pulse length (number of cycles per pulse) at 1 MHz, 300 kPa and a PRF of 100 Hz. Transfection efficacy was calculated as the percentage of fluorescent cells out of the total number of cells present. Viability was calculated as the ratio of cell densities between cells treated with and without ultrasound. Maximal transfection (0.87%) occurred with 50 cycle pulses and corresponded to 24% viability (n≥5, results expressed as mean +/− S.D., * indicates $p < 0.05$).
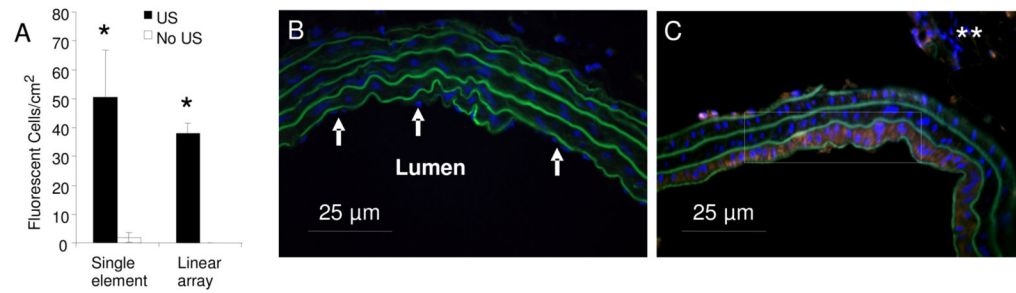
Figure 10.
Successful gene transfection using a clinical ultrasound scanner (linear array) in contrast pulse sequence mode. A) Fluorescent cell densities representing gene transfection induced by the Panametrics single element transducer or the clinical Sequoia 15L8 linear array transducer were significantly greater than fluorescent densities resulting without ultrasound (* indicates $p < 0.05$) 3.6 cells/cm^2). B, C) DAPI (blue) stained cross sections of the rat carotid balloon angioplasty model following ultrasound-mediated delivery of plasmid DNA. The contralateral control carotid artery (B) (no RFP gene expression) and the injured left carotid (RFP evident -white box). (BLUE = nuclei, GREEN = elastic lamina, RED = red fluorescent protein, ** indicates sectioning artifact)

Table 1

The number of cycles and the pulse repetition rate (PRF) for each pulsing scheme are listed. Duty cycles during transmit were kept constant for all pulsing schemes.

# of Cycles	1	10	50	100
PRF (Hz)	5000	500	100	50
Duty Cycle (% on)	0.5	0.5	0.5	0.5